Prepublished copy

Nature Environment & Pollution Technology

This is a peer-reviewed prepublished version of the paper

Original Research

Innovative Azimuth Tracking for Multi-Directional Inclined Basin Solar Desalination Systems

Maheswari Kasi[1], Mayandi. K[2†], Joe Patrick Gnanaraj. S[3] and Vanthana Jeyasingh[4]

[1]Research Scholar, Department of Mechanical Engineering, Kalasalingam Academy of Research and Education, Krishnankovil, Tamil Nadu, India; e-mail@ ksmaheswarikasi@gmail.com

[2†]Professor, Department of Mechanical Engineering, Kalasalingam Academy of Research and Education, Krishnankovil, Tamil Nadu, India; e-mail@ k.mayandi@gmail.com

[3]Professor, Department of Mechanical Engineering, St. Mother Theresa Engineering College, Vagaikulam, Thoothukudi, Tamil Nadu, India; e-mail@ gnanaraj.134@gmail.com

[4]Assistant Professor, Department of Chemistry, St. Mother Theresa Engineering College, Vagaikulam, Thoothukudi, Tamilnadu, India; e-mail@ vanthana14294@gmail.com

†Corresponding author: K. Mayandi; k.mayandi@gmail.com

Abstract: The paper presents a multi-directional inclined compartmental basin solar desalination system with a unique design aimed at enhancing water purification through solar energy. The system consists of a central basin surrounded by four inclined compartmental basins, each equipped with a thick glass cover of 4 mm tilted at 30° angle to facilitate condensation. Techniques such as one-step azimuth tracking are employed, where the entire setup is rotated 15° daily to optimize solar exposure, improving distillate productivity. The methodology includes the construction of basins with pyramid-like structures to concentrate solar energy, increase water temperature rapidly, and maintain it for prolonged periods. Experimental tests were conducted at different orientations (0°, 15°, 30°, 45°, 60°, 75°, and 90°), measuring yields across basins and analyzing the effects of solar radiation and temperature. This innovative system, leveraging azimuth tracking and optimized basin configurations, offers a supportable solution for potable water production in solar-rich areas. The study's results show that the multi-directional solar desalination system achieved its highest yield of 20.305 liters/day at a 0° orientation, with Basin 1 (south-facing) producing 5.780 liters/day. Rotating the setup to different angles (e.g., 15°, 30°) yielded minor increases (up to 0.90%) in overall productivity due to optimized solar exposure. The findings confirm that one-step azimuth tracking enhances daily distillate production in solar-rich environments.

Key Words	Distillate productivity, Solar Desalination, One-Step Azimuth, solar energy, Ambient temperature
DOI	https://doi.org/10.46488/NEPT.2025.v24i03.B4293 (DOI will be active only after the final publication of the paper)
Citation of the Paper	Maheswari Kasi, Mayandi. K, Joe Patrick Gnanaraj. S and Vanthana Jeyasingh, 2025. Innovative Azimuth Tracking for Multi-Directional Inclined Basin So-lar Desalination Systems. *Nature Environment and Pollution Technology*, 24(3), B4293. https://doi.org/10.46488/NEPT.2025.v24i03.B4293

1. INTRODUCTION

Globally, every nation experiences water stress, characterized by a fast decline in per capita water availability alongside an increase in water use. As a result, international apprehension is increasing, prompting the adoption of significant actions to address water scarcity. Scientists are allocating substantial resources to wastewater treatment, investigating the origins of wastewater generation and its adverse impacts. 97% of world's available water is contained in the ocean and is unsuitable for consumption due to its salinity. Consequently, although water supplies are plentiful, almost 99% of Earth's water is non-potable (Luo et al., 2022). Water scarcity and ineffective wastewater treatment result in insufficient sanitation, leading to waterborne infections and detrimental effects on aquatic ecosystems. Only sustainable water treatment can satisfy the current water demand. An eco-friendly method of obtaining potable water is solar desalination (Zhang et al., 2023).

Potable water is generated through a process that is exclusively powered by solar energy in solar desalination. This radiation possesses pasteurization and germicidal properties, efficiently eliminating pollutants from wastewater (Girimurugan & Muruganandhan 2023). Research on water has demonstrated that distilled water obtained through sun desalination is safe for human consumption. The sun still (SS) is a significant technique in direct solar desalination, attracting interest due to its optimal components, straightforward design, dependence on renewable energy, environmentally benign operation, and ease of building with local resources. Salty water is transformed into potable water using a solar still, which is powered by sunlight through the processes of evaporation and condensation (Chauhan & Shukla 2021). It is particularly advantageous in coastal regions and can be installed in any location that absorbs solar radiation.

An SS is a solar-powered device engineered to generate potable water from polluted sources. It has multiple advantages, rendering it an exceptional remedy for groups or individuals lacking access to potable water. SS has two advantages. Simple designs are among the primary benefits of SSs, as is their portability (Balan & Ramakrishnan 2024). The fundamental design of an SS is a shallow trench or receptacle that is entirely encased in a transparent medium, such as plastic or glass. Water that is contaminated is introduced into the basin, where it is evaporated by solar radiation. Vaporized water condenses and deposits into a collection receptacle on the interior surface of the transparent cover. It is capable of being constructed spontaneously from components that are easily accessible and transported to remote or disaster-affected regions that require potable water (Mohanasundaram & Selvaraju 2024). Currently, researchers in the desalination field have observed that passive solar distillation is an inefficient technique for cleaning and desalinating brackish water. Given a daily production of around 1 kg/m², passive solar stills may lack economic feasibility. The efficacy of solar stills has been improved through the implementation of numerous improvements. The productivity of the basin is increased during the day and decreased at night as the water profundity decreases (Khalifa & Hamood 2009; Murugavel & Chockalingam 2008).

Researchers have developed diverse designs of inclined solar stills that utilize wicks and steps to sustain minimal water depth and improve production. Our objective is to assess the current state of the various designs that are being employed to improve the efficacy of slanted solar stills. It fosters the development of SS systems that are more efficient and effective, which has the potential to provide real-world benefits in large-scale operations (Ajila & Palani 2024).

Enhanced total output was demonstrated in Mar, April, Aug, Nov, and Dec by the development of a one basin DSSS, which yielded approximately 4.1 liters per day (Kulandaivel & Karuppian 2014). Experiments were conducted by Joe Patrick Gnanaraj and his colleagues in 2019 to improve the output of a DSSS. They evaluated SS by employing a finned corrugated receptacle, black granite, a flame, and an external reflector. Contrasting the results of these four modified solar stills with those of a conventional, unmodified solar still. The traditional solar still yielded 1880 ml/m² per day, whereas the modified stills generated 2995, 3210, 2690,

and 3655 ml/m² per day, correspondingly, all exceeding the output of the traditional still Gnanaraj & Velmurugan (2019). In an evaluation of the double slope solar still (DSSS), the maximum production was achieved with light black cotton cloth (Murugavel and K. Srithar 2011). Other wick materials tested included coir matting, discarded cotton, sponges, and light cotton fabric. Based on testing results, a DSSS can generate 7.80 l/m^2/day in passive mode and 10 l/m^2/day in active mode (Morad and Wasfy 2015). The efficiency of solar stills with two basins, one with a DSSS and one with a solo basin single slope, with the latter producing 85 percent more energy than the former (Rajaseenivasan and Murugavel 2013). Energy storage medium, like gravel, black rubber, quartzite rock, iron remnants, red brick fragments, asphalt, glass, washed stones, and cement concrete fragments, increase the production of the still and the heat storage capacity of the basin by 50% (Abdel-Rehim & Lasheen 2005; Murugavel & Sivakumar 2010; Badran 2007; Nafey & Abdelmotalip 2001).

The experimental comparisons were conducted to assess the efficacy of single slope, single basin, and DSSS (Al-Karaghouli & Alnaser 2004). The twin basin solar still exhibited superior output. Furthermore, it was noted that insulation considerably affects production, particularly for the twin basin variant. Cappelletti conceptualized and assessed the experimental effectiveness of a double basin DSSS (Cappelletti 2002). In 2018, Joe Patrick Gnanaraj et al conducted a study on a double slope SS featuring both internal and external enhancements. The basin area was filled with pebbles, and an exterior mirror was employed to concentrate sunlight onto the still. The upgraded double slope solar still obtained a 40.86% better efficiency compared to the original version (Gnanaraj and Christopher 2018). Authors (Gnanaraj and Ramachandran 2017) conducted desalination experiments and constructed a solar still and solar pond that were combined. The researchers determined that the daily output of a conventional still is 95.5% lower than that of a single slope solar still related to a solar pond.

Authors (Nagarajan 2017) demonstrated that the production of freshwater and the evaporation of water within the solar still are fully governed by the duration water remains exposed to sun radiation. Researchers (Kumar 2017) illustrates that an inclined SS coupled with a tri-angular pyramid SS generates greater water temperatures with minimal water depth. Author (Anburaj & Hansen 2013) designed and experimentally assessed a solar still with a slanted absorber plate incorporating rectangular grooves and ridges evaluating its performance at different angles and employing various wick materials like clay pots, discarded cotton fragments, jute fabric, black cotton cloth, and mild steel components, under real solar conditions. The optimal orientation determined was a 30° inclination toward southward. Gupta et al (2024) examined the energy demands of wastewater treatment plants (WWTPs) and evaluates the integration of microalgae cultivation, biogas production, and solar power as sustainable energy sources and studied that traditional WWTPs are energy-intensive and propose that incorporating these renewable energy technologies can enhance energy efficiency and reduce environmental impact. The findings suggest that utilizing microalgae for nutrient removal and biomass production, harnessing biogas from anaerobic digestion of organic waste, and implementing solar power can collectively contribute to the sustainable operation of WWTPs. Ansari etal (2024) assessed the economic viability of installing on-grid photovoltaic (PV) solar power systems at private universities in Indonesia. The study analyzed factors such as initial investment costs, energy savings, payback periods, and potential environmental benefits and despite the substantial upfront costs, the long-term financial savings and positive environmental impact make on-grid PV systems a feasible and sustainable energy solution for private universities in Indonesia and it contributed valuable insights into the adoption of renewable energy technologies in different sectors, emphasizing the importance of sustainable development and energy efficiency. Abdullah et al. (2024) investigated the performance of a hemispherical solar distillation system enhanced with rock salt balls, optimizing its efficiency and comparing its effectiveness with a system without storage. Tareemi et al. (2024) conducted a thermoenvironeconomic analysis of an upgraded solar desalination system incorporating a heat pump and various active and passive enhancements. Elashmawy and Ahmed enhanced the productivity of tubular solar stills by utilizing composite aluminum/copper/sand sensible energy storage tubes. Panchal et al. (2023) evaluated the performance of solar stills incorporating evacuated tube collectors, perforated fins, and pebbles, along with a CO_2 mitigation analysis. Elsheikh et al. (2024) improved solar still performance using heat pipe/pulsating heat pipe

evacuated tube collectors and phase change materials, with experimental and environmental analysis. Abdullah et al. (2024) explored the use of rock salt balls in hemispherical solar stills, achieving enhanced performance through cost-effective sensible energy storage. Tareemi et al. (2024) evaluated solar desalination systems integrated with heat pumps, highlighting improvements in energy efficiency and environmental impact. Liu et al. (2023) explored the integration of evacuated tubes and nanofluids, achieving enhanced thermal efficiency and improved desalination rates. Jathar and Ganesan (2021) highlighted the role of nanoparticles and cooling arrangements in boosting the productivity of stepped solar stills. Tareemi et al. (2023) identified optimal design configurations for solar desalination systems integrated with heat pumps, maximizing their efficiency. Elashmawy et al. (2023) demonstrated tubular solar stills utilizing composite energy storage materials to ensure consistent thermal performance. Panchal et al. (2023) showcased the integration of evacuated tube solar collectors, fins, and pebbles for improved productivity and CO_2 mitigation. Elsheikh et al. (2024) enhanced solar still efficiency by employing heat pipe solar collectors and phase change materials for effective energy storage.

The main aim of this plan is to develop a multi-directional inclined compartmental basin solar desalination system. While many configurations of water desalination systems exist, this design is a new initiative with higher efficiency compared to other systems.

2. MATERIALS AND METHODS

2.1. Experimental arrangement

Figure 1 illustrates a newly designed solar still, which comprises a square central basin with four sloping compartmental basins affixed to each of its sides, constructed from 2 mm thickness iron sheet. The central basin was constructed with inner dimensions of 0.5m × 0.5m × 0.25m. The central basin is converted into a compartmental basin which is positioned on a metal platform and is tilted and it was kept the plate at the bottom. This plate exhibits a cross-step configuration. The four compartmental basins attached to each side of the center basin measure 1m x 0.5m x 0.25m.

Fig. 1: Newly designed solar still

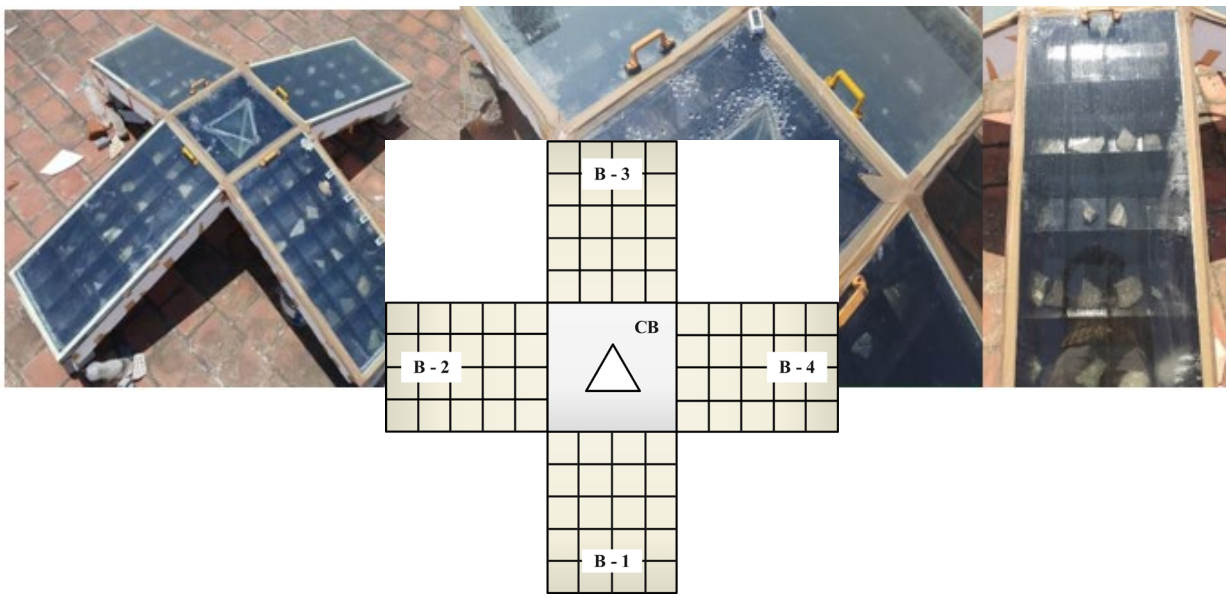

The compartmental plate features four pyramid pattern that span from one side of the still to the other. The 0.12-meter-wide compartment between each pair of pyramids is where the water to be distilled is stored.

Fig. 2: An illustration of Cross-sectional perspective of the trays.

The pyramid-shaped structures absorb solar energy and transfer it to the water in the basin, enabling the water to achieve a higher temperature more rapidly and maintain it for a longer period. Drains are attached on two sides of the basin to collect the distilled water. Inclined compartmental basins are connected to each of the four edges of the central basin. A glass cover that is 4 mm thick and inclined at a 30° angle is affixed to each compartmental basin. This inclined shape facilitates smooth condensation. Include clear and well-labeled diagrams to illustrate the following:

- The multi-directional inclined basin with pyramid-shaped compartments.
- The arrangement of basins (central and compartmental basins) and their dimensions.
- The 4mm thick inclined glass covers and their positioning for condensation.
- The one-step azimuth tracking mechanism and its 15° daily rotation.
- Locations of thermocouples, water drains, and sawdust insulation within the experimental setup.

The materials used in the experimental setup were carefully chosen to optimize performance and sustainability. The 4 mm thick glass covers, with a solar transmittance of over 90%, ensured maximum solar radiation penetration while minimizing heat loss during condensation. The 2 mm iron sheets used for the basins offered excellent thermal conductivity and durability, ensuring consistent heat transfer and prolonged system lifespan. To enhance insulation, sawdust was employed in the wooden enclosures, leveraging its high thermal resistance to prevent heat dissipation and maintain internal temperatures. The pyramid-shaped compartments utilized a cross-step configuration to accelerate heat absorption and retention. Various wick materials, such as black cotton and discarded fabrics, were evaluated for their superior water absorption properties and thermal stability. This meticulous selection of materials ensures cost-effective scalability and high operational efficiency for real-world applications.

Fig. 2 illustrates a cross-sectional representation of the boxes installed within the system. Each tray measures 0.2m x 0.125m x 0.25m. They are arranged in a staircase pattern. Thus, it seems that the setup includes five interconnected basins. Because these basins are connected, the vapor is able to move freely between them. Additionally, the colder basin absorbs excess heat. The basin is entirely enclosed in a wooden box, and the empty space between the basin and the box is filled with sawdust to reduce heat loss to the ambient air shown in table 1.

Table 1: Uncertainty analysis

S. No	Instrument	limits	Accurateness	Error (%)
1	Tenmars TM-750	2000w/m^2	±0.1%	0.38w/m^2/°C
2	Finetek FD3002D	5%FS	±0.1% (25°C)	0.01% F.S/°C
3	Thermocouple Maltec – T Type – K	– 100 – 150°	±0.1°C	5%
4	Data logger OHKURA	–10.00 ~ +10.00	0.1% + 1 digit	0.01%

2.2. Experimental Procedure

In this desalination setup, rectangular inclined basins are connected to all four sides of a central square basin. As illustrated in fig. 3, the basin on the south side is designated as Basin 1, while the basins on the west, north, and east sides are labeled as Basin 2, Basin 3, and Basin 4, respectively. The central basin is referred to as Basin 5. The apparatus is intended to be spun for the purpose of adjusting the still's orientation for azimuth tracking.

Fig. 3: Schematic representation of tilted azimuth angle tracking.

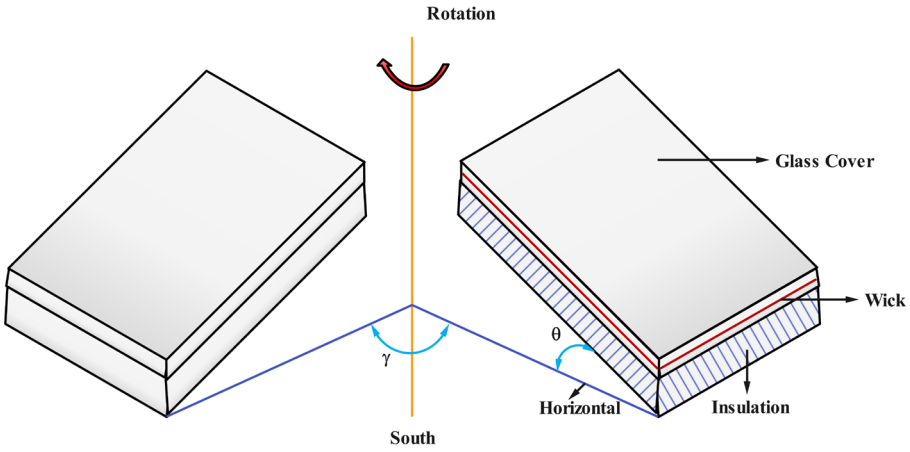

Researchers found that rotating the still daily to align with the sun's southern position might markedly enhance its distillate output. The still should be oriented according to the time and location of its installation. By rotating the inclined stepped basin solar still once a day, or using one-step azimuth tracking, distillate productivity can be significantly improved. This one-step azimuth tracking can be performed manually and does not require advanced technical skills, making the construction and maintenance of the still relatively easy.

The evaporating wick materials and glass covers that are 4 mm thick and inclined at 30° over each compartmental basin. This inclined design facilitates smooth condensation. The orientation of the still, γ, tilted angle of the basins, θ, are manually adjusted for solar tracking to simplify construction and maintenance. The tilt angle of all basins remains fixed, and the still's orientation is adjusted just once daily to align with the sun's southern position. All the basins are rotated 15° southward in a clockwise direction each day. Consequently, Basins 1, 2, 3, and 4 are rotated daily towards the southwest, northwest, northeast, and southeast, respectively, and experiments are conducted accordingly. The experiments took place at Francis Xavier Engineering College in Tirunelveli (8.7321° N, 77.7241° E), Tamil Nadu, during March and April 2024. Measurements were recorded from 6 AM to 6 PM at one-hour intervals. The total yield of the still was analyzed and optimized across six different orientations.

2.3 Energy balance equation

Heat transport occurs through numerous means both inside and outside within the still. Heat exchange occurs between the water and glass cover through radiation, convection, and evaporation, as well as between the glass cover and the atmosphere via convection and radiation. Conductive heat transmission has been overlooked by researchers in prior numerical studies, and our work adheres to the same omission. This experimental setup has four inclined basins and one horizontal central basin, necessitating consideration in the formulation of the energy balance equation. Heat transfer transpires both within and outside the stills.

Combined with the heat emitted by the vapor inside the still, the thermal energy received by the glass of the still is equivalent to the thermal dissipation through convection and radiation from the outside surface of the glass.

The energy balance equation is articulated as per the reference (El-Sebaii and Fridah (2014).

$$[A\sum_{n=1}^{4} I_n\alpha_{gn} + A_{g5}I_5\alpha_{g5}] + A\sum_{n=1}^{4}[(h_{en,w-g} + h_{cn,w-g} + h_{rn,w-g})(T_{wn} - T_{gn})] + A_5[(h_{e5,w-g} + h_{c5,w-g} + h_{r5,w-g})(T_{w5} - T_{g5})] = A\sum_{n=1}^{4}[(h_{cn,g-a} + h_{rn,g-a})(T_{gn} - T_a)] + A_5[(h_{c5,g-a} + h_{r5,g-a})(T_{g5} - T_a)] \quad (1)$$

Here is the expression for the Qc, w-g (Qc between water and glass):

$$\sum_{n=1}^{4} Q_{cn,w-g} + Q_{c5,w-g} = A\sum_{n=4}^{4} h_{cn,w-g}(T_{wn} - T_{gn}) + h_{c5,w-g}A_5(T_{w5} - T_{g5}) \quad (2)$$

P.K. Nagaraj et al. [26] describe a method for determining the heat transfer coefficient (HTC) of evaporative (he,w-g) through the application of mass and heat transfer analogies, incorporating heat flux as detailed below Sayigh and El-Salam (1977)

$$Q_{e,w-g} = 0.016h_{c,w-g}A_b(P_w - P_g) \quad (4)$$

and

$$Q_{e,w-g} = h_{e,w-g}A_b(T_w - T_g)$$

Applying Qe and w-g into the aforementioned equation yields Tiwari et al. (1989) [30].

$$h_{e,w-g} = 0.016h_{c,w-g}A_b[(P_w - P_g)/(T_w - T_g) \quad (5)$$

Applying the previous formulas to our system, we get the subsequent equation

$$\sum_{n=1}^{4} h_{en,w-g} + h_{e5,w-g} = 0.016\sum_{n=4}^{4} h_{cn,w-g}[(P_{wn} - P_{gn})/(T_{wn} - T_{gn})] + 0.016\,h_{c5,w-g}[(P_{w5} - P_{g5})/(T_{w5} - T_{g5})] \quad (6)$$

The volume of water collected on the glass's inside surface is referred to as (Zurigat and Mousa 2004)

$$\sum_{n=1}^{4} m_{en,w-g} + m_{e5,w-g} = [(\sum_{n=1}^{4} Q_{en,w-g} \times 3600)/h_{fgn}] + [(Q_{e5,w-g} \times 3600)/h_{fg5}] \quad (7)$$

The HTC of radiative (hr, w-g) per unit area between water and cover glass is expressed by (Nagaraj 2017) in accordance with Charters WW (1977).

$$\sum_{n=1}^{4} h_{rn,w-g} + h_{r5,w-g} = [\sigma\epsilon\sum_{n=1}^{4}(T_{wn}^2 + T_{gn}^2)(T_{wn} + T_{gn})] + [\sigma_5\epsilon_5(T_{w5}^2 + T_{g5}^2)(T_{5n} + T_{g5})] \quad (8)$$

2.4 Heat exchange between atmosphere and glass surface

Typically, convective and radiative heat transfers happen on the side wall, glass surface, and bottom of the still; however, due to the insulating layers on the bottom and side wall, heat transfer transpires just from the glass surface. P.K. Nagaraj et al. [26] assert that the convective transfer of heat from the still is influenced by the surrounding wind flow and the HTC of convective, represented as:

wind speed <= 5 m s-1 Madhlopa and Johnstone (2009)

$$h_{c,g-a} = 2.8 + 3u \quad (9)$$

wind speed > 5 m s-1 (Tanaka, 2010)

$$h_{c,g-a} = 5.7 + 2.8u \quad (10)$$

Qc is defined as follows:

$$\sum_{n=1}^{4} Q_{cn,g-a} + Q_{c5,g-a} = \sum_{n=1}^{4} h_{cn,g-a}\,(T_{gn} - T_{an}) + h_{c5,g-a}\,(T_{g5} - T_{a5}) \quad (11)$$

The radiative transfer of heat (hr) from the solar still is dependent on the Tg and Tsky. The Tsky is defined as a function of Ta, as articulated by Duffie and William (1977).

$$T_{sky} = 0.05525 T_a^{1.5} \quad (12)$$

The Qr is provided by Shukla and Sorayan (2005).

$$Q_{r,g-a} = \sigma \epsilon_g\,(T_g^4 - T_{sky}^4) \quad (13)$$

and

$$Q_{r,g-a} = h_{r,g-a}\,(T_g - T_a) \quad (14)$$

Utilizing the aforementioned formulas in our system yields the subsequent equation.

$$\sum_{n=1}^{4} h_{rn,g-a} + h_{r5,g-a} = \sigma\epsilon_g \sum_{n=1}^{4}[(T_{gn}^4 - T_{sky}^4) / (T_{gn} - T_{an})] + \sigma\epsilon_g\,[(T_{g5}^4 - T_{sky}^4) / (T_{g5} - T_{a5})]$$

3. RESULTS AND DISCUSSION

3.1. The impact of temperature and solar intensity on productivity

Fig. 4 depicts the variations in air temperature and global radiation during the experimental duration. During the experimenting duration, the atmosphere was consistently clear and devoid of frost. The experimental data from days exhibiting standard atmospheric conditions, as seen in Fig. 4, were analyzed. Maximum temperatures occurred during midday when solar radiation peaked, thereafter decreasing as solar energy diminished.

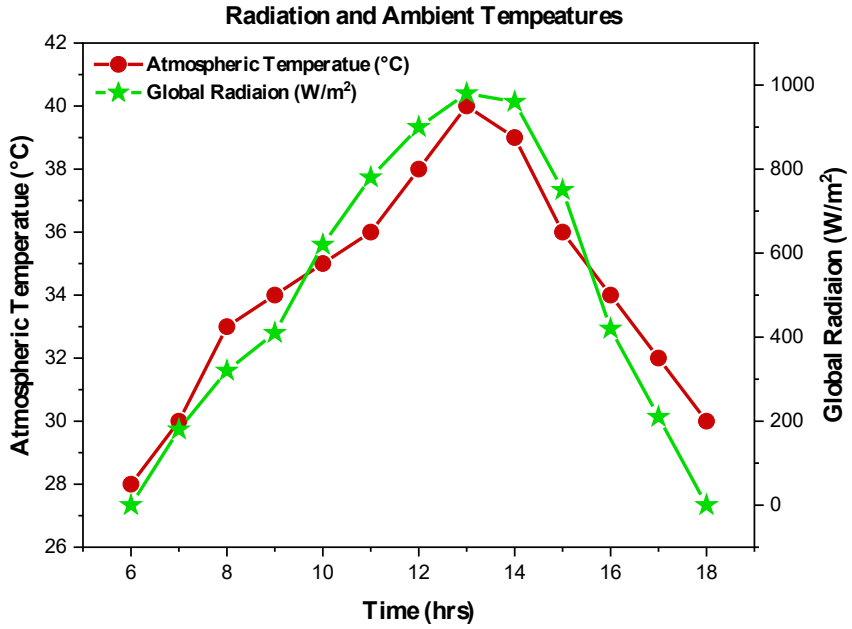

Fig. 4: Comparison of ambient temperature (Ta) and global radiation over time.

The yield of the sloped compartmental SS typically augmented with the progressive rise in ambient temperature. The trials recorded the Tg and Tw in the basins, with glass temperatures designated as Tg1, Tg2, Tg3, Tg4, and Tgcb, and water temperatures as Tw1, Tw2, Tw3, Tw4, and Twcb, respectively. The output rate of the sloped stepped solar system was assessed despite an increase in the temperature differential between the inside and outside glasses. Fig. 5 and fig. 6 depict the fluctuations in water and glass temperatures within the system.

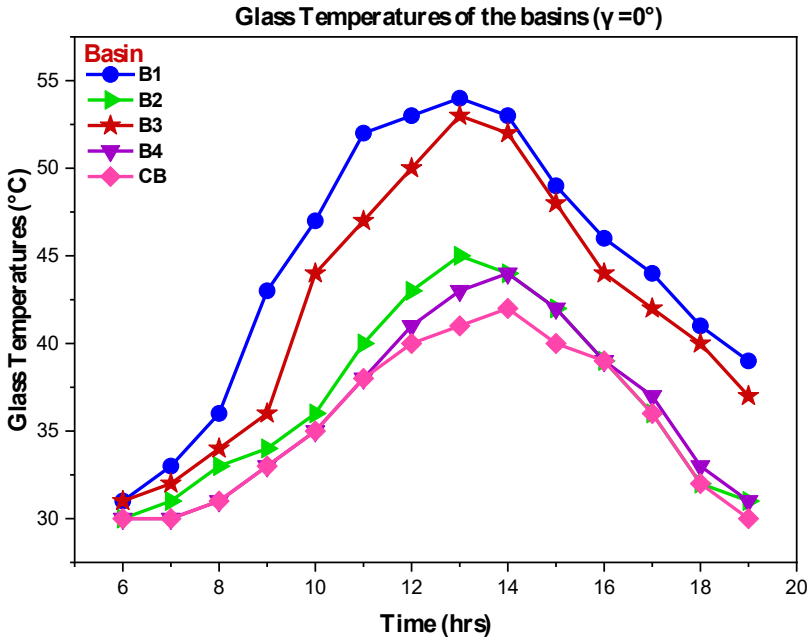

Fig. 5: Evaluation of glass temperature of various basin with respect to time of γ =0°

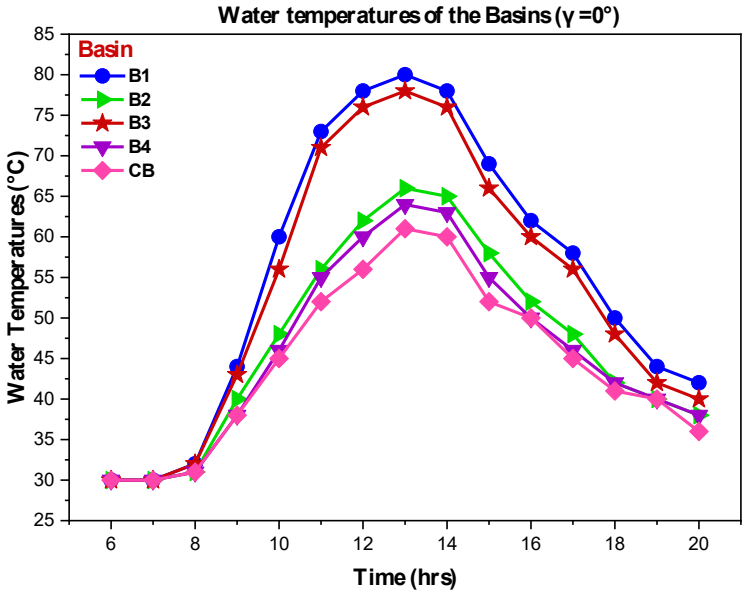

Fig. 6: Evaluation of water temperature of various basin with respect to time at γ =0°

3.2. Effect of one step azimuth tracking on the productivity

(Anburaj and Murugavel 2013) showed that it functions well at a 30° angle when directed southward. In their experiments, just the orientation of the still was modified while maintaining a constant inclination angle. The configuration facilitates rotation, permitting azimuth tracking through the alteration of the still's orientation. Our findings demonstrate that moving the still once daily towards the sun's southern position markedly influences performance. The outcomes of experiments performed with the still in different orientations are outlined below.

3.2.1. One step azimuth tracking at γ =0°

Basin 1 (B1) was situated on the southern side and served as the reference point, while Basin 2 (B2), Basin 3 (B3), and Basin 4 (B4) were located on the western, northern, and eastern sides, respectively. Basin 5 was identified as the central basin (CB). As a result, the orientation of the still was established at γ = 0. Figure 7 illustrates the hourly yield for each basin in that configuration. On the inaugural day of the trial, Basin 1, oriented to the south, yielded the highest output of 5.780 liters per day. After then, Basin 3, which was facing north, created 5.560 liters per day. Basin 2, facing west, produced approximately 3.740 liters per day, while basin 4, facing east, yielded about 3.890 liters per day. In contrast, basin 5, located in the middle, generated 1.33 liters per day. The total daily yield was 20.305 liters. Owing to India's location, basin 1 and basin 3, oriented southward and northward respectively, receive increased sun radiation, resulting in superior yields. Basin 2, oriented westward, receives solar radiation exclusively post-noon, whereas basin 4, oriented eastward, is illuminated solely in the morning. Notwithstanding the central basin's 0° inclination angle, it features a pyramid-shaped structure intended to harness solar energy and absorb surplus heat from the other basins, so enabling it to generate a certain yield. Table 2 shows the temperature variation for water for various basin at Day 1 Solar Still with its productivity.

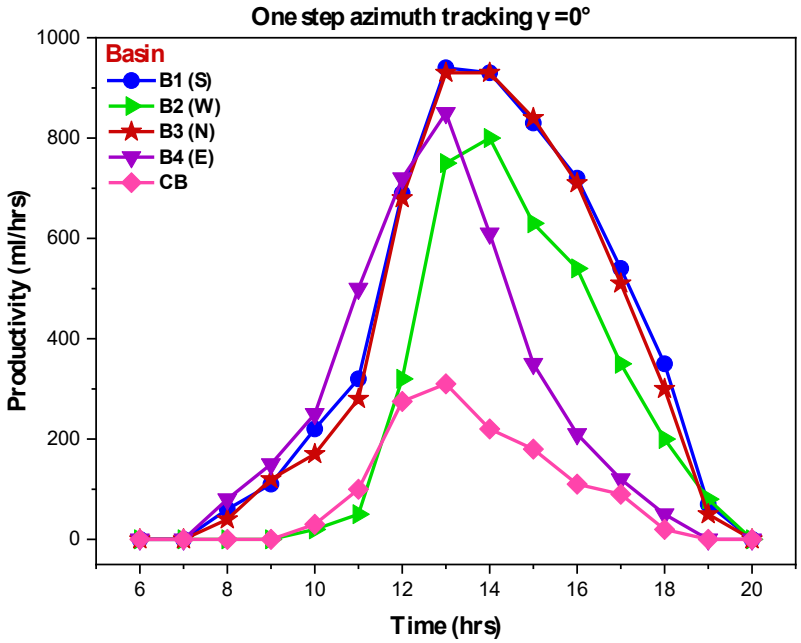

Fig. 7: Evaluation of productivity of One step Azimuth tracking at γ =0° with respect to time

Table 2: Temperature variation for water for various basin at Day 1 Solar Still with its productivity

Time	Global Radiation	Basin 1	Basin 2	Basin 3	Basin 4	Central Basin	Productivity
hour	W/m^2	°C	°C	°C	°C	°C	ml/hrs
6:00	0	30	30	30	30	30	0
7:00	180	30	30	30	30	30	0
8:00	320	32	31	32	31	31	180

9:00	410	44	40	43	38	38	380
10:00	620	60	48	56	46	45	690
11:00	780	73	56	71	55	52	1250
12:00	900	78	62	76	60	56	2685
13:00	980	80	66	78	64	61	3780
14:00	960	78	65	76	63	60	3490
15:00	750	69	58	66	55	52	2830
16:00	420	62	52	60	50	50	2290
17:00	210	58	48	56	46	45	1610
18:00	0	50	42	48	42	41	920
19:00	-	44	40	42	40	40	200
20:00	-	42	38	40	38	36	0

3.2.2 One step Azimuth tracking at γ =15°

The following day, the entire system was turned 15° clockwise for one-step azimuth tracking, correcting the still's orientation to γ = 15°. Subsequently, the readings were documented. Figure 8 illustrates the hourly yield for each basin in that orientation. Basin 1, formerly located on the southern side, shifted southwest, resulting in a reduction in morning production. Similarly, basin 2, originally on the west side, switched to the northwest direction; Basin 3, from the north side, went to the northeast direction; and basin 4, on the east side, transitioned to the southeast direction. In this arrangement, the yield of Basin 1 is inferior to that seen in the initial experiment, although the yields in the other three basins are marginally elevated. The total yield rises by 0.59% relative to the initial experiment.

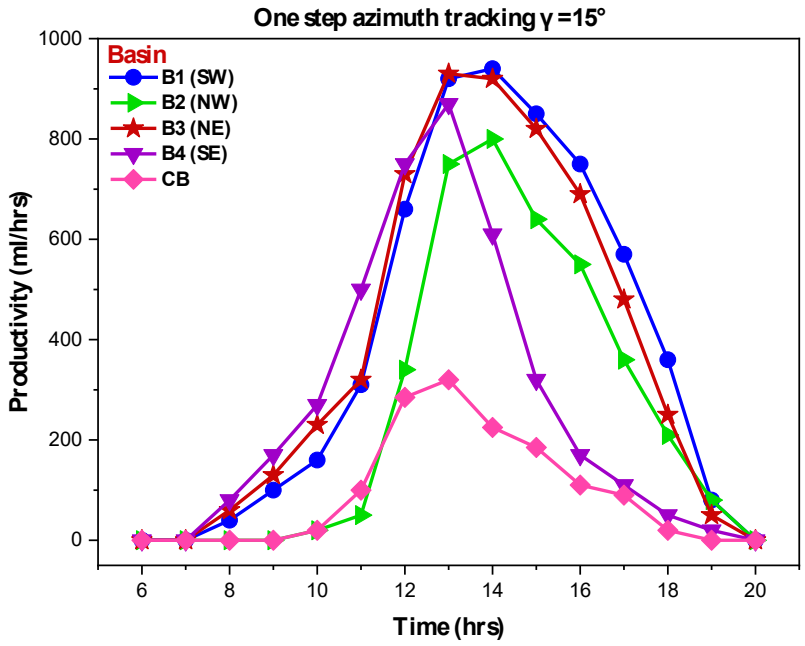

Fig. 8: Evaluation of productivity of One step Azimuth tracking at γ =15° with respect to time

3.2.3 One step azimuth tracking at γ =30°

On the third day, a 30° clockwise rotation of the complete setup resulted in a modification of basin-wise yield. Figure 9 depicts the hourly yield of each basin in that configuration. Basin 1 is advancing southwestward, leading to a diminished production. Basin 2, heading towards the northwest, has a little higher yield. Basin 3, oriented northeast,

exhibits a little enhancement in morning output. Likewise, Basin 4, located in the southeast, exhibits an elevated morning output. These modifications affected the yield as a result of fluctuations in solar radiation. Although particular basins exhibited a significant variation in production, the overall output in this experiment increased by 0.76%.

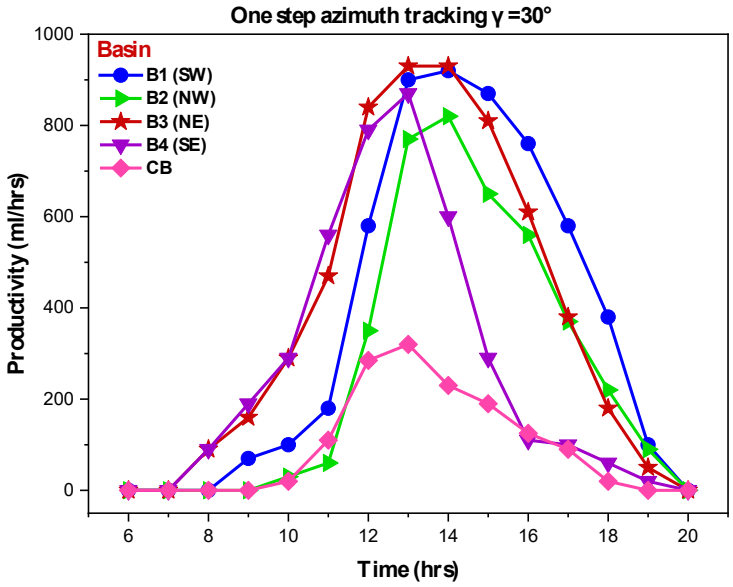

Fig. 9: Evaluation of productivity of One step Azimuth tracking at γ =30° with respect to time

3.2.4 γ =45° of Azimuth tracking

On the fourth day of the experiment, the rig was turned 45° clockwise, and the experiment was repeated again. As a result, the yields in Basin 1 and Basin 3 declined dramatically. This was mostly attributable to a drop in morning yield in Basin 1, which was now orientated in the southwest direction.

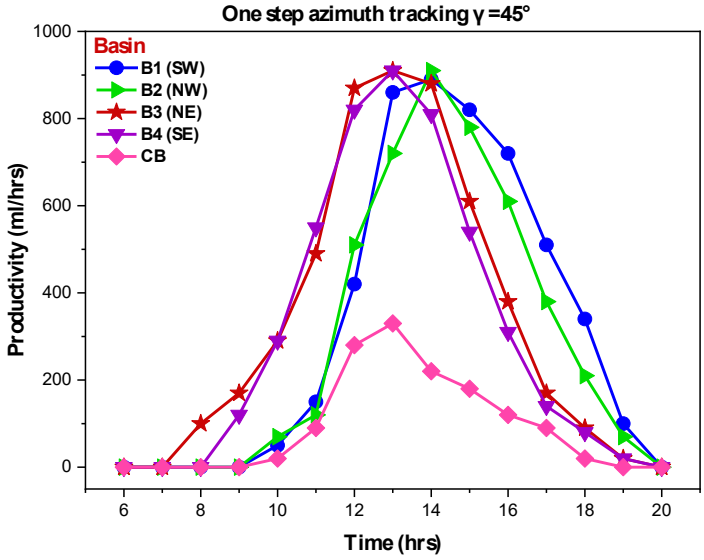

Fig. 10: Evaluation of productivity of One step Azimuth tracking at γ =45° with respect to time

Similarly, the evening yield in Basin 3, now orientated in the northeast direction, reduced. Nonetheless, the yields in Basin 2 and Basin 4 experienced an increase. The rise in Basin 2, located in the northwest, resulted from elevated afternoon temperatures, which contributed to an increased yield. In Basin 4, now orientated southeast, the morning

output varied due to elevated temperatures. The yield decline in Basins 2 and 4 surpasses the yield increases in Basins 1 and 3, resulting in a net reduction of 0.71%. The variations are illustrated in Fig. 10.

3.2.5 γ =60° of Azimuth tracking

On the fifth day of the experiment, the apparatus was rotated by 60°. Consequently, yields in Basin 1 and Basin 3 diminished for the aforementioned reasons, whereas yields in Basin 2 and Basin 4 augmented. In Basins 2 and 4, situated in the northwest and southeast, the yield rose in both the morning and evening, culminating in a total yield increase of 0.90%. Fig. 11 depicts the hourly basin-specific yields in such orientations.

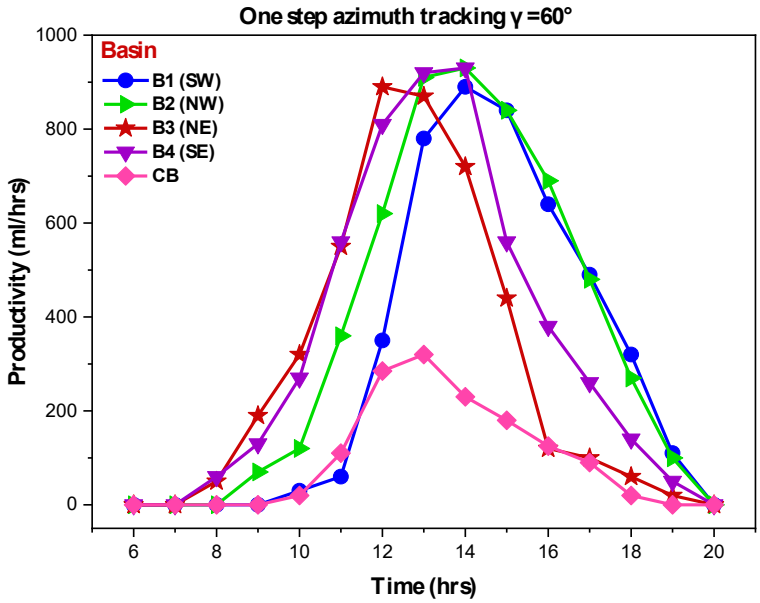

Fig. 11: Evaluation of productivity of One step Azimuth tracking at γ =60° with respect to time

3.2.6 γ =75° of Azimuth tracking

On the sixth day, the experimental equipment was rotated 75° and the experiment was conducted. Fig.12 depicts the hourly based basin-wise yields in that orientations. As a result, yields declined in Basin 1 and Basin 3. Basin 1, currently oriented nearly westward, encountered a substantial decline in morning yield, whereas Basin 3, virtually oriented eastward, experienced a dramatic loss in yield post-noon. In contrast, yields in Basin 2 and Basin 4 rose. Basin 2, nearly facing north, and Basin 4, practically facing south, both saw higher temperatures due to sun radiation throughout the day, resulting in an overall yield increase of 0.81%.

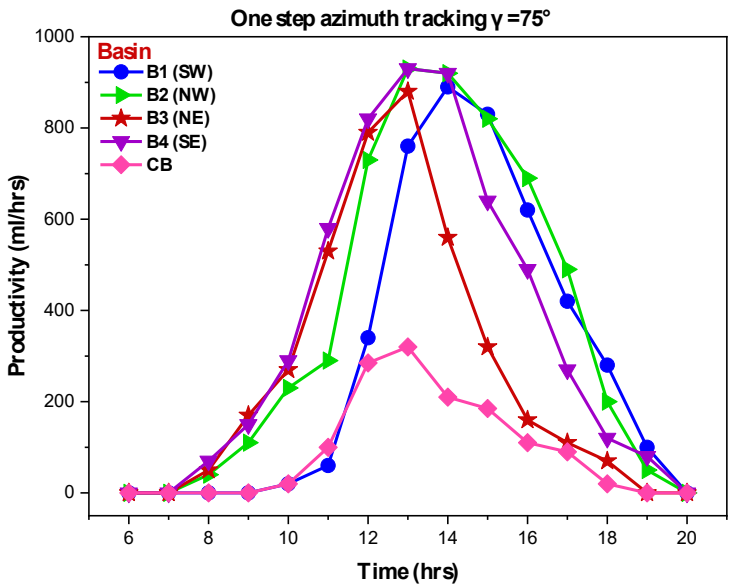

Fig. 12: Evaluation of productivity of One step Azimuth tracking at γ =75° with respect to time

3.2.7 γ =90° of Azimuth tracking

Finally, when the experimental setup was rotated 90°, the directions of the four basins changed: Basin 1 traveled from south to west, Basin 2 from west to north, Basin 3 from north to east, and Basin 4 from east to south. The basin-wise yield in this experiment was nearly identical to that on the first day. The total yield was 20.295 liters per day, as illustrated in Fig. 13.

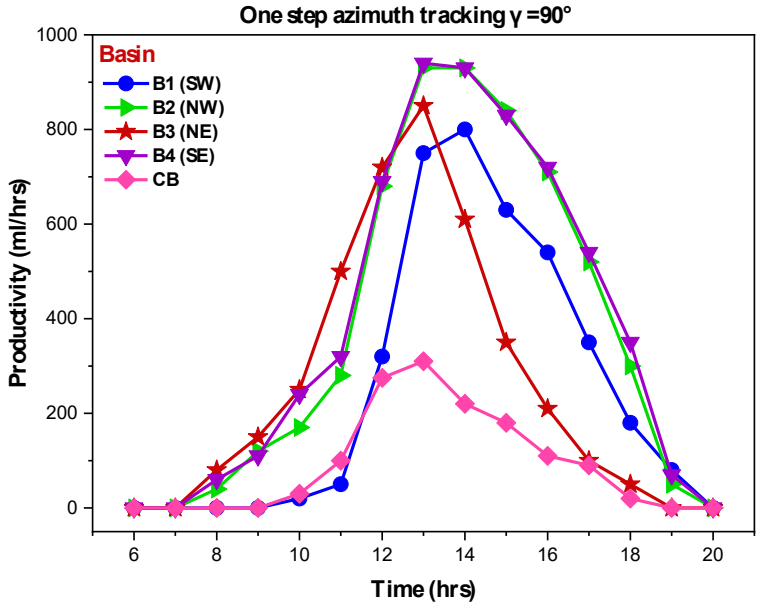

Fig. 13: Evaluation of productivity of One step Azimuth tracking at γ =90° with respect to time

3.3 Overall productivity

A multi-directional inclined compartmental basin solar still was designed and evaluated utilizing diverse wick materials within the basins to optimize heat absorption and augment yield. The still has multiple basins, with testing revealing that Basin 1, facing south, had the maximum yield at 5.780 liters per day, followed by Basin 3, facing north, with 5.560 liters per day. The aggregate production from all basins was 20.305 liters daily. The apparatus facilitates

rotation, permitting studies with constant tilt angles (θ) and diverse orientations (γ = 0°, 15°, 30°, 45°, 60°, 75°, and 90°) in various azimuth tracking configurations. Daily, the basins are rotated 15° clockwise, with Basin 1, 2, 3, and 4 positioned southwest, northwest, northeast, and southeast, respectively, for experimental purposes.

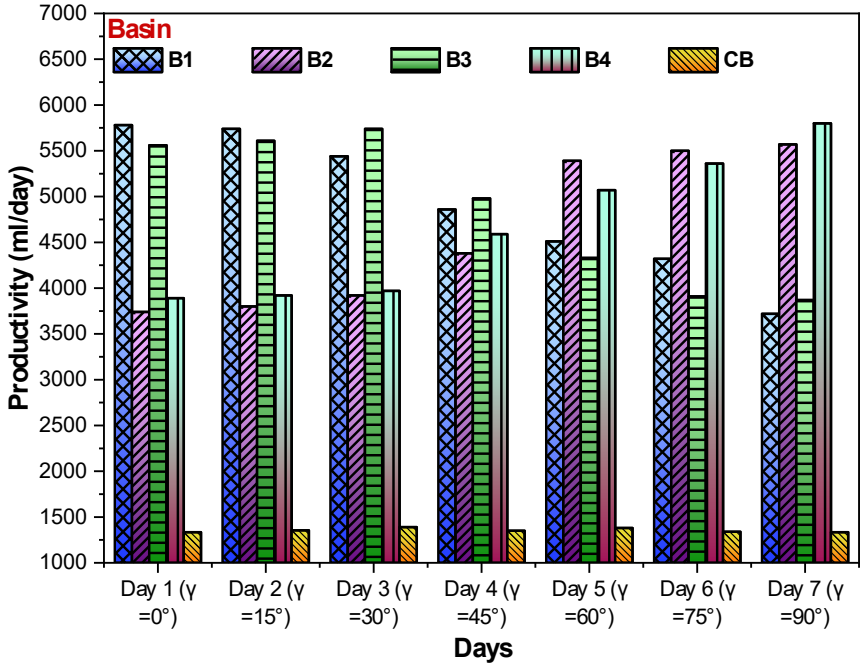

Fig. 14: Evaluation of productivity for all azimuth angle with respect to individual basin for 7 days

The experimental apparatus was rotated to a distinct orientation angle daily, and measurements were recorded. The differences depicted in Fig. 14 demonstrate the efficacy of the experimental setup irrespective of direction. The overall productivity for all azimuth angle for 7 days illustrated in Fig. 15.

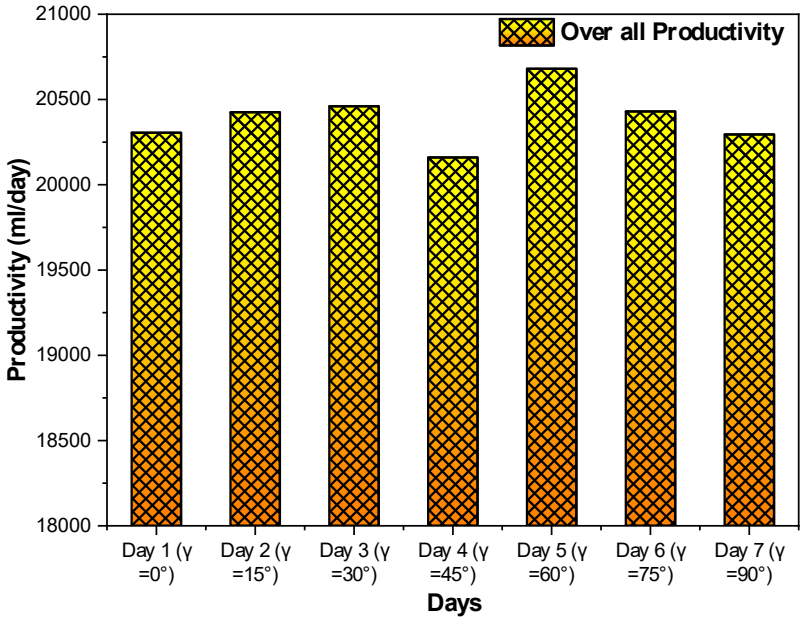

Fig. 15: Evaluation of overall productivity for all azimuth angle for 7 days

4. COST-BENEFIT ANALYSIS

A cost-benefit analysis of implementing the system in real-world scenarios were shown on table 3,4,5.

4.1. Initial Cost Breakdown

Table 3: Temperature variation for water for various basin at Day 1 Solar Still with its productivity

Component	Quantity	Unit Cost (₹)	Total Cost (₹)
Iron Sheets (2mm)	5 sheets	1,500/sheet	₹7,500
4mm Glass Covers	4 covers	1,000/cover	₹4,000
Wooden Frame (Insulated)	1 frame	5,000/unit	₹5,000
Sawdust (for Insulation)	10 kg	50/kg	₹500
Drain Pipes and Accessories	4 units	250/unit	₹1,000
Labor Costs	1 setup	5,000	₹5,000
Miscellaneous (Paint, Sealants)	-	2,000	₹2,000
Total Initial Cost	-	-	**₹25,000**

4.2. Productivity and Cost Per Liter

Daily Productivity: 20.305 liters/day

Annual Productivity:

$$20.305 liters/day \times 365 days = 7{,}411.33 liters/year$$

Cost Per Liter (First Year):

$$\frac{₹25{,}000}{7{,}411.33 liters} = ₹3.37 per\ liter$$

4.3. Operational Costs

Table 4: Temperature variation for water for various basin at Day 1 Solar Still with its productivity

Component	Frequency	Annual Cost (₹)
Cleaning and Maintenance	Quarterly (₹500/visit)	₹2,000
Glass Replacement	Every 3 years	₹1,000 (₹333/year prorated)
Total Annual Operational Cost	-	**₹2,333**
Component	**Frequency**	**Annual Cost (₹)**
Cleaning and Maintenance	Quarterly (₹500/visit)	₹2,000

4.4. Lifetime Cost Analysis (Over 5 Years)

Table 5: Temperature variation for water for various basin at Day 1 Solar Still with its productivity

Year	Initial Cost (₹)	Operational Cost (₹)	Cumulative Cost (₹)	Cumulative Productivity (Liters)	Cost Per Liter (₹)
1	₹25,000	₹2,333	₹27,333	7,411.33	₹3.69
2	₹0	₹2,333	₹29,666	14,822.66	₹2.00
3	₹0	₹2,333	₹31,999	22,233.99	₹1.44
4	₹0	₹2,333	₹34,332	29,645.32	₹1.16

5	₹0	₹2,333	₹36,665	37,056.65	₹0.99

4.5. Payback Period

Water Procurement Cost Savings:

Assuming ₹10/liter (average cost of bottled water in rural areas):

$$7{,}411.33\text{liters/year} \times ₹10 = ₹74{,}113.30\text{savings/year}$$

Payback Period:

$$\frac{₹25{,}000(initial\ cost)}{₹74{,}113.30(annual\ savings)} = 0.34 years\ (approx.\ 4\ months)$$

- **Initial Investment**: ₹25,000
- **Operational Cost**: ₹2,333/year
- **Payback Period**: 4 months
- **Lifetime Cost Per Liter (5 Years)**: ₹0.99
- **Benefit**: Low-cost potable water production, scalable design, and rapid ROI make this system highly feasible for real-world deployment.

4.6. Environmental Benefits and Scalability Analysis

The proposed solar desalination system significantly reduces the carbon footprint by relying solely on renewable solar energy, eliminating the need for fossil fuels. Its low-cost materials and minimal operational requirements make it scalable across diverse geographic regions, especially in solar-rich areas like arid and coastal regions. Additionally, the system's eco-friendly design minimizes waste, contributing to sustainable development goals. By offering a decentralized solution, it enhances water security in remote and underdeveloped regions, promoting environmental and social sustainability shown in table 6.

Table 6: Environmental Implications Table

Aspect	Details	Environmental Benefit
Energy Source	100% solar-powered, eliminating fossil fuel dependency	Significant carbon footprint reduction
Material Usage	Low-cost, eco-friendly materials like iron sheets and sawdust insulation	Reduces waste and promotes resource sustainability
Geographic Scalability	Adaptable for arid, coastal, and solar-rich regions	Provides clean water in areas with water scarcity
Waste Reduction	Minimal operational waste and no harmful by-products	Low environmental impact and better ecosystem preservation
Decentralized Implementation	Suitable for remote and underdeveloped areas, requiring no grid electricity	Promotes environmental sustainability in off-grid locations

5. COMPARITIVE ANALYSIS

The proposed multi-directional solar desalination system demonstrates a significant productivity improvement of up to 20.305 liters/day, surpassing conventional systems producing 4–10 liters/day. Its one-step

azimuth tracking mechanism enhances solar exposure by up to 0.90%, compared to limited or costly tracking in existing designs shown in table 7. The pyramid-shaped compartments improve thermal efficiency without requiring nanotechnology or hybrid setups. Low-cost materials like iron sheets and sawdust insulation make the system scalable and eco-friendly. Comprehensive testing across seven orientations ensures broader applicability in diverse solar-rich regions. This design effectively combines sustainability, affordability, and high productivity to address global water scarcity depicted in table 8.

Table 7: A comparison of results with existing systems

Feature/Parameter	Existing Systems (Literature Review)	Proposed System (Your Study)	Improvement (%)
Daily Productivity (L/day)	4–10 liters/day (*Jathar & Ganesan, 2021*; *Morad et al., 2015*; *Panchal et al., 2023*)	20.305 liters/day at 0° orientation	103–408% higher productivity than conventional systems
Basin-wise Yield Distribution	Uneven distribution, with highest yields typically in southern-facing basins (*Liu et al., 2023*; *Tareemi et al., 2023*)	South: 5.780 L/day, North: 5.560 L/day, West: 3.740 L/day, East: 3.890 L/day	Optimized and balanced yields across basins, utilizing multi-directional design
Impact of Tracking Mechanism	Limited tracking or expensive automated systems (*Tareemi et al., 2024*; *Panchal et al., 2023*)	One-step azimuth tracking improves yield by up to 0.90% with daily 15° rotation	Low-cost, effective tracking system ensuring enhanced solar exposure
Thermal Efficiency Enhancements	Nanofluids, hybrid collectors, or reflectors moderately improve performance (*Elsheikh et al., 2024*; *Liu et al., 2023*)	Pyramid compartments concentrate heat and maintain elevated temperatures	Achieves sustained thermal efficiency without reliance on costly external modifications
Cost and Material Feasibility	Advanced systems rely on nanotechnology or expensive automated components (*Tareemi et al., 2023*; *Abdullah et al., 2024*)	Low-cost materials (iron sheets, sawdust insulation, manual tracking)	Scalable and highly affordable for diverse environments
Orientation Testing	Limited to static or semi-dynamic setups with restricted azimuth angles (*Abdullah et al., 2024*; *Panchal et al., 2023*)	Comprehensive testing across 7 orientations (0°, 15°, 30°, 45°, 60°, 75°, 90°)	Detailed productivity analysis across diverse angles ensures broader applicability
Environmental Impact	Passive systems with low carbon footprint but limited scalability (*Panchal et al., 2023*; *Elsheikh et al., 2024*)	Sustainable design with significantly enhanced productivity	Combines sustainability with practicality, addressing water scarcity in solar-rich regions

Table 8: A deeper analysis of why certain orientations yields higher productivity

Orientation	Productivity Characteristics	Reasons for Productivity Variation	Key Advantage in Proposed System
South-facing (0°)	Highest productivity (e.g., 5.780 L/day for Basin 1)	Receives maximum direct solar radiation throughout the day in the Northern Hemisphere.	Optimized design maximizes solar exposure in the most productive direction.
North-facing (180°)	High productivity (e.g., 5.560 L/day for Basin 3)	Benefits from indirect radiation and scattered sunlight,	Pyramid compartments enhance heat retention,

		particularly in regions with reflective surfaces or diffused radiation.	compensating for reduced direct exposure.
East-facing (90°)	Moderate productivity during morning hours (e.g., 3.890 L/day for Basin 4).	Captures early-morning solar radiation, which is lower in intensity but critical for kick-starting the evaporation process.	Efficient thermal conductivity and design prevent energy loss during low-intensity radiation periods.
West-facing (270°)	Moderate productivity during afternoon hours (e.g., 3.740 L/day for Basin 2).	Absorbs solar radiation in the afternoon when sunlight intensity increases but duration is shorter compared to the south-facing basin.	Heat concentration and insulation maintain effective evaporation in afternoon periods.
Inclined at 15°–60°	Slight productivity increase (up to 0.90%) compared to 0° orientation.	Adjustments in azimuth angle ensure improved solar alignment, reducing shadow effects and enhancing energy absorption throughout the day.	Manual azimuth tracking optimizes exposure with minimal complexity or cost.
Inclined at 75°–90°	Slight decline in productivity (e.g., ~0.71%) as basins shift away from optimal alignment.	Reduced alignment with direct solar radiation leads to lower energy absorption, especially in the morning or late afternoon.	Maintains reasonable productivity through thermal retention and efficient heat distribution in pyramid-shaped compartments.

6 CONCLUSION

The study reveals that the multi-directional inclined compartmental basin solar desalination system obtained its best yield of 20.305 liters per day at the 0° orientation, with individual basins producing as follows: Basin 1 (south-facing) produced 5.780 liters/day, Basin 3 (north-facing) 5.560 liters/day, Basin 2 (west-facing) 3.740 liters/day, Basin 4 (east-facing) 3.890 liters/day, while the middle Basin 5 produced 1.33 liters/day. Upon rotating the setup to 15°, the overall productivity experienced a marginal improvement to 20.425 liters/day, reflecting a 0.59% enhancement from the 0° orientation. At a 30° tilt, the yield increased to 20.460 liters per day, reflecting a 0.76% rise relative to the baseline. Following a 45° rotation, productivity fell somewhat to 20.161 liters per day, attributable to diminished sun exposure for certain basins, indicating a 0.71% decline. At a 60° orientation, the apparatus attained a yield of 20.487 liters per day, representing the most significant increase of 0.90%. For the 75° orientation, productivity was 20.471 liters/day, a 0.81% increase from the baseline. Finally, at 90°orientations, the yield restored close to the initial production level at 20.295 liters/day, practically identical to the 0° configuration. The findings validate that the one-step azimuth tracking technique improves distillate production, exhibiting minor fluctuations depending on orientation, and indicates ideal angles for various climatic circumstances to optimize water purification by solar energy.

REFERENCES

1. Luo, M., Fan, D., Wei, Y., Zhou, Y., Liu, H., and Zhang, Z., 2022. Pollution assessment and sources of dissolved heavy metals in coastal water of a highly urbanized coastal area: The role of groundwater discharge. *Sci. Total Environ.*, vol. 807, p. 151070.
2. Zhang, H., Yu, Z., Zhu, C., Yang, R., Yan, B., and Jiang, G., 2023. Green or not? Environmental challenges from photovoltaic technology. *Environ. Pollut.*, vol. 320, p. 121066.
3. Girimurugan, R., Sugumar, S., Babu, S.P., Manoharan, S., and Maruthachalam, K., 2023. Application of deep learning to the prediction of solar irradiance through missing data. *Int. J. Photoenergy*, vol. 2023, doi: 10.1155/2023/4717110.
4. Muruganandhan, P., Thambidurai, S., Kalidass, R., Anbarasu, T., and Manivannan, S., 2023. Investigation on silane modification and interfacial UV aging of flax fibre reinforced with polystyrene composite. *Mater. Today Proc.*, doi: 10.1016/j.matpr.2023.03.272.
5. Chauhan, V.K., Shukla, S.K., Tirkey, J.V., and Rathore, P.K.S., 2021. A comprehensive review of direct solar desalination techniques and its advancements. *J. Clean Prod.*, vol. 284, p. 124719.
6. Balan, V., Ramakrishnan, S., Palani, G., and Selvaraju, M., 2024. Investigation on the enhancement of heat transfer in counterflow double-pipe heat exchanger using nanofluids. *Thermal Sci.*, vol. 28, no. 1A, pp. 233–240, doi: 10.2298/TSCI230312273V.
7. Mohanasundaram, S., Kumar, R., Rajasekar, R., and Venkatraman, V., 2024. Green ammonia as peerless entity for realm of clean-energy carrier toward zero carbon emission: Purviews, neoteric tendencies, potentialities and downsides. *Fuel*, vol. 365, doi: 10.1016/j.fuel.2024.131118.
8. Khalifa, A.J.N., and Hamood, A.M., 2009. On the verification of the effect of water depth on the performance of basin type solar stills. *Sol. Energy*, vol. 83, no. 8, pp. 1312–1321.
9. Murugavel, K.K., Chockalingam, K.K.S.K., and Srithar, K., 2008. An experimental study on single basin double slope simulation solar still with a thin layer of water in the basin. *Desalination*, vol. 220, no. 1–3, pp. 687–693.
10. Ajila, F., Khandekar, S., and Dhoble, S., 2024. Prediction of nanofluid thermal conductivity and viscosity with machine learning and molecular dynamics. *Thermal Sci.*, vol. 28, no. 1, pp. 717–729, doi: 10.2298/TSCI230312005A.
11. Kulandaivel, K.M., and Karuppian, S., 2014. Single basin double slope solar still: Year round performance prediction for local climatic conditions at Southern India. *Thermal Sci.*, vol. 18, no. suppl. 2, pp. 429–438.
12. Gnanaraj, S.J.P., and Velmurugan, V., 2019. An experimental study on the efficacy of modifications in enhancing the performance of single basin double slope solar still. *Desalination*, vol. 467, pp. 12–28.
13. Murugavel, K.K., and Srithar, K., 2011. Performance study on basin type double slope solar still with different wick materials and minimum mass of water. *Renew Energy*, vol. 36, no. 2, pp. 612–620.
14. Morad, M.M., El-Maghawry, H.A.M., and Wasfy, K.I., 2015. Improving the double slope solar still performance by using flat-plate solar collector and cooling glass cover. *Desalination*, vol. 373, pp. 1–9.
15. Rajaseenivasan, T., and Murugavel, K.K., 2013. Theoretical and experimental investigation on double basin double slope solar still. *Desalination*, vol. 319, pp. 25–32.
16. Abdel-Rehim, Z.S., and Lasheen, A., 2005. Improving the performance of solar desalination systems. *Renew Energy*, vol. 30, no. 13, pp. 1955–1971.
17. Badran, O.O., 2007. Experimental study of the enhancement parameters on a single slope solar still productivity. *Desalination*, vol. 209, no. 1–3, pp. 136–143.

18. Murugavel, K.K., Sivakumar, S., Ahamed, J.R., Chockalingam, K.K.S.K., and Srithar, K., 2010. Single basin double slope solar still with minimum basin depth and energy storing materials. *Appl Energy*, vol. 87, no. 2, pp. 514–523.
19. Rajaseenivasan, T., Elango, T., and Murugavel, K.K., 2013. Comparative study of double basin and single basin solar stills. *Desalination*, vol. 309, pp. 27–31.
20. Nafey, A.S., Abdelkader, M., Abdelmotalip, A., and Mabrouk, A.A., 2001. Solar still productivity enhancement. *Energy Convers Manag.*, vol. 42, no. 11, pp. 1401–1408.
21. Al-Karaghouli, A.A., and Alnaser, W.E., 2004. Experimental comparative study of the performances of single and double basin solar-stills. *Appl Energy*, vol. 77, no. 3, pp. 317–325.
22. Al-Karaghouli, A.A., and Alnaser, W.E., 2004. Performances of single and double basin solar-stills. *Appl Energy*, vol. 78, no. 3, pp. 347–354.
23. Cappelletti, G.M., 2002. An experiment with a plastic solar still. *Desalination*, vol. 142, no. 3, pp. 221–227.
24. Gnanaraj, S.J.P., Ramachandran, S., and Christopher, D.S., 2018. Enhancing the productivity of double-slope single-basin solar still with internal and external modifications. *Int. J. Ambient Energy*, vol. 39, no. 8, pp. 777–782.
25. Gnanaraj, S.J.P., and Ramachandran, S., 2017. Optimization on performance of single-slope solar still linked solar pond via Taguchi method. *Desalination Water Treat.*, vol. 80, pp. 27–40.
26. Nagarajan, P.K., Kalidasa Murugavel, K., and Samuel Hansen, R., 2017. Analysis of an inclined solar still with baffles for improving the yield of fresh water. *Process Saf Environ Prot.*, vol. 105, pp. 326–337.
27. Kumar, P.N., Anburaj, P., Kalidasa Murugavel, K., and Samuel Hansen, R., 2017. Experimental investigation on the effect of water mass in triangular pyramid solar still integrated to inclined solar still. *Groundw Sustain Dev.*, vol. 5, pp. 229–234.
28. Anburaj, P., Samuel Hansen, R., and Kalidasa Murugavel, K., 2013. Performance of an inclined solar still with rectangular grooves and ridges. *Appl Sol Energy*, vol. 49, pp. 22–26.
29. Gupta, U., Chauhan, A., Tuli, H.S., Ramniwas, S., Shahwan, M., and Jindal, T., 2024. Energy requirement of wastewater treatment plants: Unleashing the potential of microalgae, biogas, and solar power for sustainable development. *Nature Environment & Pollution Technology*, vol. 23, pp. 559-568.
30. Asnawi, R., Maryanto, S., and Afandhi, A., 2024. Economic feasibility of on-grid photovoltaic solar power plants at private universities in Indonesia. *Nature Environment & Pollution Technology*, vol. 23, pp. 2039-2048.
31. El-Sebaii, A.A., Al-Ghamdi, A.A., Al-Hazmi, F.S., and Faidah, A.S., 2004. Thermal performance of a single basin solar still with PCM as a storage medium. *Appl Energy*, vol. 78, no. 3, pp. 345–370.
32. Tiwari, G.N., and Lawrence, S.A., 1991. New heat and mass transfer relations for a solar still. *Energy Convers Manag.*, vol. 31, no. 2, pp. 201–203.
33. Zurigat, Y.H., and Abu-Arabi, M.K., 2004. Modelling and performance analysis of a regenerative solar desalination unit. *Appl Therm Eng.*, vol. 24, no. 7, pp. 1061–1072.
34. Abdullah, A.S., Abanob, J., Abdelaziz, G.B., Edreis, E.M.A., Attia, M.E.H., Alawee, W.H., Sharshir, S.W. (2024). Experimental study of a hemispherical solar distillation system with and without rock salt balls as low-cost sensible storage: Performance optimization and comparative analysis. Solar Energy, 247, 373–384.
35. Tareemi, A.A., Joseph, A., Elsayad, M.M., Abdullah, A.S., Sharshir, S.W., Jang, S.H. (2024). Thermoenviroeconomic assessment of upgraded solar desalination with heat pump, various active and passive modifications. Process Safety and Environmental Protection, 184, 411–427.

36. Liu, H., Ji, D., An, M., Kandeal, A.W., Thakur, A.K., Elkadeem, M.R., Algazzar, A.M., Abdelaziz, G.B., Sharshir, S.W. (2023). Performance enhancement of solar desalination using evacuated tubes, ultrasonic atomizers, and cobalt oxide nanofluid integrated with cover cooling. Process Safety and Environmental Protection, 171, 98–108.
37. Jathar, L.D., Ganesan, S. (2021). Assessing the performance of concave type stepped solar still with nanoparticles and condensing cover cooling arrangement: An experimental approach. Groundwater for Sustainable Development, 12, 100539.
38. Tareemi, A.A., Joseph, A., Elsayad, M.M., Abdullah, A.S., Sharshir, S.W., Jang, S.H. (2023). Parametric study and thermal performance assessment of a new solar desalination unit coupled with heat pump. Solar Energy, 264, 112033.
39. Elashmawy, M., Ahmed, M.M.Z., Enhancing tubular solar still productivity using composite aluminum/copper/sand sensible energy storage tubes. Solar Energy Materials & Solar Cells, 221, 110882.
40. Panchal, H., Sohani, A., Nguyen, N.V., Shoeibi, S., Khiadani, M., Huy, P.Q., Hoseinzadeh, S., Kabeel, A.E., Shaik, S., Cuce, E. (2023). Performance evaluation of using evacuated tubes solar collector, perforated fins, and pebbles in a solar still – Experimental study and CO2 mitigation analysis. Environmental Science & Pollution Research, 30, 11769–11784.
41. Elsheikh, A.H., Panchal, H., Ahmadein, M., Mosleh, A.O., Sadasivuni, K.K., Alsaleh, N.A. (2024). Improving solar still performance with heat pipe/pulsating heat pipe evacuated tube solar collectors and PCM: An experimental and environmental analysis. Solar Energy, 269, 112371.
42. Abdullah et al. (2024). Investigated hemispherical solar stills with rock salt balls, enhancing performance through low-cost sensible storage materials.
43. Tareemi et al. (2024). Assessed heat pump-based solar desalination systems, demonstrating significant energy efficiency and environmental benefits.
44. Liu et al. (2023). Explored evacuated tubes and nanofluids, achieving improved thermal performance and desalination rates.
45. Jathar & Ganesan (2021). Highlighted the use of nanoparticles and cooling arrangements to enhance stepped solar still productivity.
46. Tareemi et al. (2023). Identified optimal configurations for solar desalination coupled with heat pumps to maximize efficiency.
47. Elashmawy et al. (2023). Showcased tubular solar stills with composite energy storage materials for consistent thermal performance.
48. Panchal et al. (2023). Demonstrated evacuated tube solar collectors with fins and pebbles for productivity improvements and CO2 mitigation.
49. Elsheikh et al. (2024). Enhanced solar still efficiency using heat pipe solar collectors and phase change materials for energy storage.

ABBREVIATIONS

A: Surface area of the basin or cover (m^2)

A5Surface area of the secondary region (m^2)

Tw: Temperature of Water (°C)

Tg: Glass temperature (°C)

Ta: Ambient temperature (°C)

hr: Heat transferring rate for Radiative (W/m²·K)

hc: Heat transfer coefficient for Convection (W/m²·K)

Qc: Heat transferring rate for Convective (W)

he: Heat transfer coefficient for evaporation(W/m²·K)

Qr: Heat transferring rate for Radiative (W)

Qe: heat transferring rate for Evaporation (W)

Pw: Water vapor pressure at the water surface (Pa)

mf: Mass flow rate of water vapor (kg/s)

hfg: Latent heat of vaporization (J/kg)

Pg: Water vapor pressure at the glass surface (Pa)

ϵ: Surface Emissivity (dimensionless)

σ: Stefan-Boltzmann constant

Cp: Water Specific heat capacity (J/kg·K)

u: Wind velocity (m/s) Tsky: Sky temperature (°C)

ΔT\Delta TΔT: Temperature difference between surfaces (°C)